J. Phys. Chem. A **2003,** *107,* 8763−8773

Electron-Withdrawing Effects on Metal−Olefin Bond Strengths in $Ni(PH_3)_2(CO)(C_2X_nH_{4-n})$, $X = F$, Cl; $n = 0-4$: A DFT Study

Darin N. Schlappi and David L. Cedeño*

Department of Chemistry, Illinois State University, PO Box 4160, Normal, Illinois 61790-4160

Received: June 20, 2003; In Final Form: August 19, 2003

Density functional theory (DFT) studies have been performed in the title complexes to determine the effect of electron-withdrawing halogens around the C═C bond on the metal−olefin bond dissociation energy. Calculations indicate that the nickel−olefin bond dissociation energy would be nearly independent of the number of electron-withdrawing elements around the double bond. The results are explained in terms of electronic, steric, and reorganizational effects that derive from the olefin−metal interaction and are compared to computational and experimental results for related complexes, which show similar metal−olefin bond strength behavior. It has been found that reorganizational effects in both the olefin and $Ni(PH_3)_2(CO)$ play a determining role in the overall bond dissociation energy trend.

Introduction

The metal−olefin bond is one of the most important ones in organometallic chemistry. Olefin−metal complexes are involved in most catalytic cycles that have been developed to transform olefins into highly functionalized products, including olefin hydrogenation, isomerization, hydrocarbonylation, epoxidation, polymerization, etc.[1−5] From a thermodynamic perspective, the viability of these reactions depends on the relative strengths of the bonds involved. Given that the metal−olefin bond is involved in these processes, a complete understanding of how the metal and its coordinated ligands influence a given metal−ligand interaction is very important in the development of improved transition metal catalysts. Recent studies have provided important information about intermediate species involved in some of these reactions.[6−15] Although these studies have given insight into some mechanistic issues, it is still necessary to investigate more about fundamental thermodynamic aspects such as bond strengths.

The most common description of the metal−olefin bond was introduced by Dewar[16] and complemented by Chatt and Duncanson[17] about 50 years ago, and it is known as the Dewar−Chatt−Duncanson (DCD) model. The contributions and implications of the DCD model in organometallic chemistry have been reviewed thoroughly in recent years.[18] The model is a qualitative molecular orbital description of the bonding, viewed as a two-way synergistic electron density exchange between the metal and the olefin. According to this description, the metal−olefin bond is the result of two bonding interactions. The olefin's HOMO donates electron density to the LUMO of the unsaturated metal complex in a σ-type interaction, while the HOMO of the metal complex donates electron density back to the π^* LUMO of the olefin through a π-type interaction, referred to as back-bonding. Although this description is correct, it does not provide a complete quantitative understanding of metal−olefin bond strengths. Consider, for example, the prediction of metal−olefin bond strengths for complexes containing halogenated olefins ($X_2C{=}CX_2$, where X = F or Cl) relative to ethylene ($H_2C{=}CH_2$). In terms of common qualitative interpretations of the Dewar−Chatt−Duncanson description, the π-bonding dominates the interaction between electron-rich metals and olefins, implying that halogenated olefins would bind to metals stronger than ethylene because they are better electron density π acceptors.[19,20] Experimental[21−23] and computational[23−26] evidence seems to indicate that such predictions are not always fulfilled. Recent studies by Cedeño and Weitz[23] showed that for the homologous series $Cr(CO)_5(X_2C{=}CX_2)$ and $Fe(CO)_4(X_2C{=}CX_2)$ the metal (M)−olefin bond strength follows the trend $M-C_2H_4 > M-C_2F_4 > M-C_2Cl_4$. Further evidence is found in the classical study performed by Tolman 30 years ago, where he reported the formation constants of (olefin)bis(tri-*o*-tolyl phosphite)nickel complexes for 38 olefins.[22] In relation to fluorinated olefins, Tolman concludes, "It is commonly believed that fluoro-olefins form more stable metal-olefin bonds than do hydrocarbons.... We were extremely surprised to find that none of the fluoro olefins examined were as good as C_2H_4 in coordinating to Ni(0)."

These experimental observations have motivated the present study, in which a systematic density functional theory study of the dependence of the Ni−olefin bond strengths on the electron-withdrawing ability of an olefin has been performed using a series of halogenated olefin complexes. Ni−olefin bond energies in the $Ni(PH_3)_2(CO)(C_2X_nH_{4-n})$ (X = F, Cl; $n = 0-4$) series of complexes have been calculated using density functional theory (DFT).

In this study, trends in the Ni−olefin bond strengths are analyzed in terms of the electronic and steric interactions of the olefin and the $Ni(PH_3)_2(CO)$ fragment as a function of the identity of the halogen (fluorine vs chlorine) and the number of halogens (i.e., the extent of electron-withdrawing ability) around the C═C bond. The analysis is done by correlating trends in the reorganizational energies of both olefin and $Ni(PH_3)_2(CO)$ to changes in geometrical parameters and orbital populations. A comparison of the results obtained in this study to related systems is also made.

---

* To whom correspondence should be addressed. E-mail: dcedeno@ilstu.edu.

10.1021/jp0357572 CCC: $25.00

TABLE 1: Calculated Bond Dissociation Enthalpies (in kcal/mol) Using Different DFT Functionals and Two Basis Sets

	B3LYP LACVP**	B3LYP LACV3P**	BLYPLACVP**	BLYPLACV3P**	BP86LACVP**	BP86LACV3P**	exptl value
Ni−CO in $Ni(CO)_4$[a]	17.3	16.3	19.6	19.1	23.5	24.1	$\sim 23^{\circ b}$ 25.0 ± 1.9^{c}
$Ni-C_2H_4$ in NiC_2H_4[d]	18.4	16.7	34.9	32.8	41.5	40.0	35.5 ± 5^{e}

[a] Relative to singlet state $Ni(CO)_3$ at 298 K. [b] Kr solution at 120 K from ref 38. [c] Gas phase from ref 39. [d] Relative to triplet state atomic nickel at 0 K. [e] Gas phase at 0 K from ref 40.

Computational Method

All density functional theory (DFT) calculations were performed using the Jaguar quantum chemistry program.[27] A benchmarking computation using the BP86, BLYP, and B3LYP methods[28−34] to calculate known Ni−L (L = CO, C_2H_4) bond enthalpies (vide infra) supports the utilization of the BP86 functional throughout the present study. Calculations were run using the LACV3P** basis set. This is a triple-ζ set employing Hay and Wadt's effective core potential (ECP)[35] to describe nickel, while the nonmetals (H, C, O, F, P, and Cl) are described using the 6-311G** basis set.[36] For all atoms the frozen core approximation was used, but the outermost core orbitals have been kept unfrozen.

Bond energies (ΔE) were calculated from the difference in the optimized energies of the ground state of the gas phase products and reactants for the reaction:

$$Ni(PH_3)_2(CO)(C_2X_nH_{4-n}) \rightarrow Ni(PH_3)_2(CO) + C_2X_nH_{4-n}\ (X = F, Cl) \quad (1)$$

$$\Delta E = E[Ni(PH_3)_2(CO)] + E[C_2X_nH_{4-n}] - E[Ni(PH_3)_2(CO)(C_2X_nH_{4-n})] \quad (2)$$

This energy, ΔE, represents the reaction energy for olefin dissociation relative to the bottom of the minimum in the potential energy curve (D_e). Thus, in terms of eq 2, factors that lead to an increase in bonding are positive and those leading to a decrease are negative.

Bond enthalpies (ΔH) at 298 K are calculated from ΔE according to the expression

$$\Delta H_{calc} = \Delta E + \Delta ZPE + \Delta E_{th} + \Delta(PV) \quad (3)$$

where ΔZPE is the zero-point energy obtained from a calculation of the vibrational frequencies; ΔE_{th} is the energy change associated with the translational, rotational, and vibrational motion when going from 0 to 298 K, and Δ(PV) is the molar work, which is equal to ΔnRT. Previous studies of iron and chromium complexes[23,26] have shown that including the basis set superposition error (BSSE) correction decreases the calculated enthalpy values to a point where they are significantly below the experimental values, without changing the trend in the calculated metal−olefin bond enthalpies; therefore BSSE corrections are not included in this study.

The bond energy (ΔE) has been decomposed in two terms:

$$\Delta E = \Delta E_{int} + \Delta E_{reorg} \quad (4)$$

In eq 4, the net interaction energy (ΔE_{int}) represents the energy required to "snap" the bond while keeping the two resulting fragments (olefin and $Ni(CO)(PH_3)_2$) at the geometries they adopt when bonded to each other. This term is positive because "snapping" the bond is an endergonic process. The reorganizational energy (ΔE_{reorg}) is the energy resulting from these fragments relaxing to their ground state. Given that the relaxation process is exergonic, ΔE_{reorg} is negative.

To establish the extent of orbital interactions in terms of changes in orbital populations, a natural bond orbital (NBO) analysis[37] was made for all the complexes. When comparing one complex to another, in the context of the calculated data, some of the energy differences are within the computational error limits. Therefore we focus on a comparison of *trends* in the calculated bond energies, and the contributions of various factors to these bond energies.

Results

Benchmarking of DFT Functionals. The choice of functional is, in many cases, dependent on the molecular system under study. Therefore, benchmarking calculations have been performed in order to decide which DFT functional would give the most reliable bond energies for the complexes under study considering that there are no experimental results available for them. The benchmarking was done using the experimentally determined Ni−L bond energies for both $(CO)_3Ni-CO$[38,39] and $Ni-C_2H_4$.[40] The BP86, BLYP, and B3LYP functionals with both LACVP** and LACV3P** basis sets were tested. Table 1 shows the results in terms of bond enthalpies as calculated using eq 3.

As can be seen from Table 1, B3LYP underestimates the metal−olefin bond energy by a large extent, therefore is not suitable. Previous studies in iron and chromium carbonyl olefin and dinitrogen complexes[26,41] show a similar trend for the B3LYP functional. Both BLYP and BP86 show better agreement with experimental values, although BP86 values are usually larger than those obtained with BLYP. The Ni−CO bond enthalpy in $Ni(CO)_4$ is reproduced better using BP86, while the BLYP seems to do a better job than BP86 in reproducing the $Ni-C_2H_4$ bond enthalpy in NiC_2H_4. In any case, both calculations agree with experiments within the experimental uncertainty. The values in Table 1 have not been corrected for BSSE, but as previously indicated, the BSSE correction tends to decrease the results below the experimental values. Thus, we may conclude that the BP86 values will be the closest to the experimental values. It is therefore the most suitable functional to be used in the present study.

Geometry of Complexes. Although, to our knowledge, there is no available experimental data on the geometry of the $Ni(PH_3)_2(CO)(C_2X_nH_{4-n})$ (X = F, Cl; n = 0−4) complexes, there are X-ray structure determinations for both $Ni(PPh_3)_2(C_2H_4)$[42] and $Ni(PPh_3)_2(CO)_2$[43] that allow us to check the reliability of the DFT/BP86 method in reproducing Ni−CO, Ni−P, C−C, and $Ni-C_{olef}$ bond lengths and P−Ni−P and P−Ni−CO angles. A comparison with calculated values for $Ni(PPh_3)_2(CO)_2$ and $Ni(CO)(PH_3)_2(C_2H_4)$ is shown in Table 2. In general, there is good agreement between the calculated and experimental parameters.

When studying the $Ni(PH_3)_2(CO)(C_2X_nH_{4-n})$ (X = F, Cl; n = 0−4) complexes, it has been taken under consideration that the position of the olefin relative to both phosphine and carbonyl ligands would generate different rotational isomers (rotamers) and stereoisomers. Rotation of the olefin in 60° intervals yields

TABLE 2: DFT/BP86-LACV3P Calculated and Experimental Bond Lengths (in Å) and Angles (in deg) for $Ni(PPh_3)_2(CO)_2$, $Ni(PPh_3)_2(C_2H_4)$, and $Ni(PH_3)_2(CO)(C_2H_4)$**

	Ni−CO	Ni−P	Ni−C_{olef}	C−O	C−C	P−Ni−CO	Ni−C−O
calcd $Ni(PPh_3)_2(CO)_2$	1.790	2.226		1.160		111.1	178.5
exptl[a] $Ni(PPh_3)_2(CO)_2$	1.763	2.221		1.142		109.4	178.2
calcd $Ni(PH_3)_2(CO)(C_2H_4)$		2.237	2.120		1.394	108.1	
exptl[b] $Ni(PPh_3)_2(C_2H_4)$		2.152	1.99		1.43	110.5	

[a] X-ray structure determination from ref 43. [b] X-ray structure determination from ref 42.

TABLE 3: Selected Geometrical Parameters Calculated for Minimum Energy $Ni(PH_3)_2(CO)(C_2X_nH_{4-n})$ (X = F, Cl; n = 0−4) Complexes[a]

	C_2H_4	C_2H_3F	iso-$C_2H_2F_2$	cis-$C_2H_2F_2$	trans-$C_2H_2F_2$	C_2HF_3	C_2F_4
Ni−C_{olef} (CH_2)	2.104 (2.135)	2.102	2.066				
Ni−C_{olef} (CHX)		2.093		2.054 (2.046)	2.032 (2.036)	2.024	
Ni−C_{olef} (CX_2)			2.027			1.992	1.976 (1.978)
$C{=}C$	1.394	1.389	1.397	1.401	1.399	1.411	1.423
P−Ni−P	108.3	108.1	106.8	104.7	106.4	106.2	105.1
Θ(HH)[b]	21.1 (20.8)	26.3			33.6		
Θ(HX)[b]		24.8	29.7 (30.1)	29.8 (30.2)		35.8	
Θ(XX)[b]					30.0	33.4	40.8 (37.8)
Δ($C{=}C$)[c]	0.058	0.059	0.063	0.065	0.064	0.075	0.087
−Δ(P−Ni−P)[c]	16.7	16.5	17.8	19.9	18.5	18.4	19.5
Ω[d]	33.6	35.9	41.4	41.4	41.1	43.5	45.2

	C_2H_3Cl	iso-$C_2H_2Cl_2$	cis-$C_2H_2Cl_2$	trans-$C_2H_2Cl_2$	C_2HCl_3	C_2Cl_4
Ni−C_{olef} (CH_2)	2.076	2.041				
Ni−C_{olef} (CHX)	2.073		2.029 (2.047)	2.016 (2.034)	2.011	
Ni−C_{olef} (CX_2)		2.013			1.999	1.985 (1.979)
$C{=}C$	1.396	1.406	1.409	1.404	1.420	1.440
P−Ni−P	106.0	103.7	102.4	103.6	102.0	99.7
Θ(HH)[b]	26.9			31.2		
Θ(HX)[b]	29.6	32.7 (30.7)	33.2 (33.4)		34.8	
Θ(XX)[b]				38.4	38.9	38.6 (37.1)
Δ($C{=}C$)[c]	0.064	0.076	0.072	0.067	0.087	0.109
−Δ(P−Ni−P)[c]	18.6	20.9	22.2	21.0	22.6	24.9
Ω[d]	38.9	46.5	48.7	46.5	50.6	55.6

[a] Bond lengths and angles in Å and deg, respectively. [b] Pyramidalization angle, defined as 180° minus the dihedral angle of trans substituents; HH refers to $H{-}C{=}C{-}H$, HX to $H{-}C{=}C{-}X$, and XX to $X{-}C{=}C{-}X$. [c] Δ($C{=}C$) is the change in $C{=}C$ bond length: bonded minus free olefin; Δ(P−Ni−P) is the change in the angle between phosphine ligands for the olefin complex minus that in $Ni(PH_3)_2(CO)$. [d] Planarity deviation of the phosphines and carbonyl ligands in the olefin complex relative to $Ni(PH_3)_2(CO)$, calculated as 360° minus the sum of CO−Ni−P and P−Ni−P angles.

CHART 1

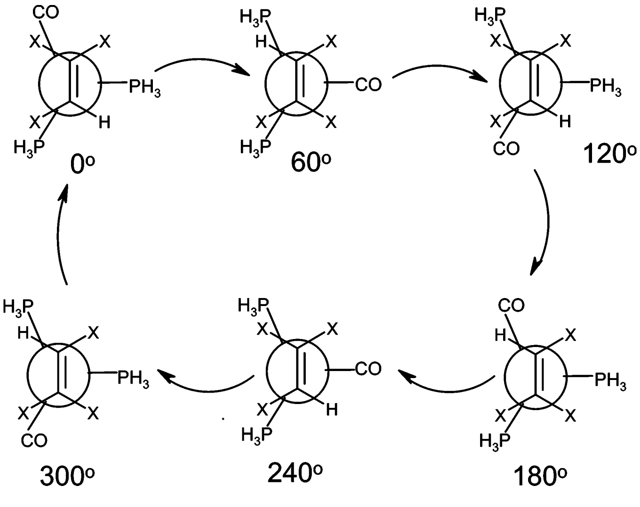

six different rotational isomers. Chart 1 depicts Newman projections of the six possible rotamers for a C_2HX_3 complex. For reference purposes, the molecules have been oriented such that the ligand perpendicular to the $C{=}C$ axis is pointing to the right (3 o'clock position). In addition, a rotamer with the $C{=}C$ axis perpendicular to any of the phosphine ligands is arbitrarily considered to be at either 0° or 180° rotation. The 0° and 180° rotamers are represented in such a way that the CO is in the 11 o'clock position, while a 120° or 300° rotamer has the CO in the 7 o'clock position. The 60° and 120° rotamers are those in which the $C{=}C$ axis is perpendicular to the C−O bond. Stereoisomers are also possible for those complexes containing two different atoms bonded to an olefinic carbon ($HXC{=}CX_2$, trans- and cis-$HXC{=}CXH$, and $H_2C{=}CXH$). This is possible because once the olefin is bonded to the metal, the olefinic carbon becomes chiral as a result of the sp^2 to sp^3 rehybridization. In the case of a complex containing a cis-$C_2H_2X_2$ olefin, the enantiomer of the 0° rotamer is the 180° rotamer, while for the trans-$C_2H_2X_2$ the 0° and 180° rotamers are identical. Geometry optimizations and energy minimizations have been carried out for all possible rotamers and stereoisomers. Table 3 shows selected parameters for the isomer of each complex that has the lowest energy (vide infra). In general Ni−CO and Ni−P bond lengths and the P−Ni−CO bond angle in the complexes are reproduced well by the calculations relative to the experimental X-ray values for $Ni(PPh_3)_2(CO)_2$ and $Ni(PPh_3)_2(C_2H_4)$, even taking into consideration that the olefin may affect these parameters due to both electronic and steric factors.

Geometry optimizations were also carried out for both the free olefins and the singlet state of the unsaturated $Ni(CO)(PH_3)_2$ complex. As expected, all olefins deviate from a planar geometry when they are bonded to the metal. This is due to partial sp^2 to sp^3 rehybridization of the olefinic carbons as a result of the back-bonding interaction. This is evidenced by both

CHART 2

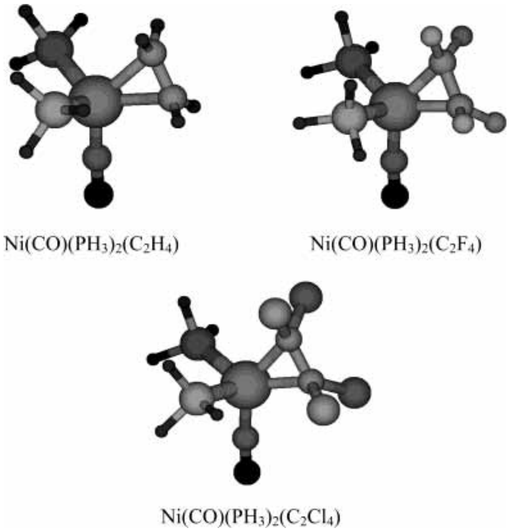
Ni(CO)(PH$_3$)$_2$(C$_2$H$_4$)

Ni(CO)(PH$_3$)$_2$(C$_2$F$_4$)

Ni(CO)(PH$_3$)$_2$(C$_2$Cl$_4$)

the elongation of the C═C bond (Δ(C═C) in Table 3) and the so-called pyramidalization angle of the olefin (notated as Θ in Table 3). A geometry optimization of ^{1}Ni(CO)(PH$_3$)$_2$ results in a trigonal planar geometry, with a P−Ni−P angle separation of 124.6°. The Ni(CO)(PH$_3$)$_2$(olefin) complexes have tetrahedral geometries (see Chart 2), in which the olefin forces the three other ligands to bend away from it. This is reflected in both the differences in the P−Ni−P angle (Δ(P−Ni−P) in Table 3) and the deviation from planarity relative to the unsaturated complex (notated as Ω in Table 3).

The bond distance between the metal and the olefinic carbons is dependent on the identity of the halogen atoms and their number in each carbon. In general, a carbon bonded to a halogen is closer to the metal than one bonded to hydrogen, while a carbon bonded to fluorine is closer to the metal than one bonded to chlorine. It is also observed that metal−olefinic carbon bond lengths gets shorter as the number of halogens around the C═C bond increases. For example, carbons in ethylene are separated by ∼2.1 Å from the metal, but are only 1.98 Å away from the metal in both the tetrahalogenated complexes.

An analysis of the geometrical trends seen for these complexes and their dependence on the nature of the olefin will be discussed later.

Nickel−Olefin Bond Energies and Enthalpies. Charts 3 and 4 show the optimized geometries and relative energies (kcal/mol) for fluorinated and chlorinated complex conformations that converged to a minimum, respectively. Table 4 summarizes energy results obtained from energy minimizations.

These results show that for both tetrahalogenated olefin complexes, the 60° rotamer converged to give the 0° rotamer, implying that this rotamer is not a minimum on their potential energy surface. However, a calculation starting with the 60° rotamer of the ethylene complex converged to a minimum that is higher in energy (∼2 kcal/mol) than the 0° rotamer.

In the case of the trihalogenated complexes, optimizations starting with the 60° or 240° rotamers converted to an isomer in which the C═C bond avoids being perpendicular to the CO ligand. The lowest energy rotamers are the ones in which two nongeminal halogens are not eclipsed with CO and PH$_3$ ligands

CHART 3

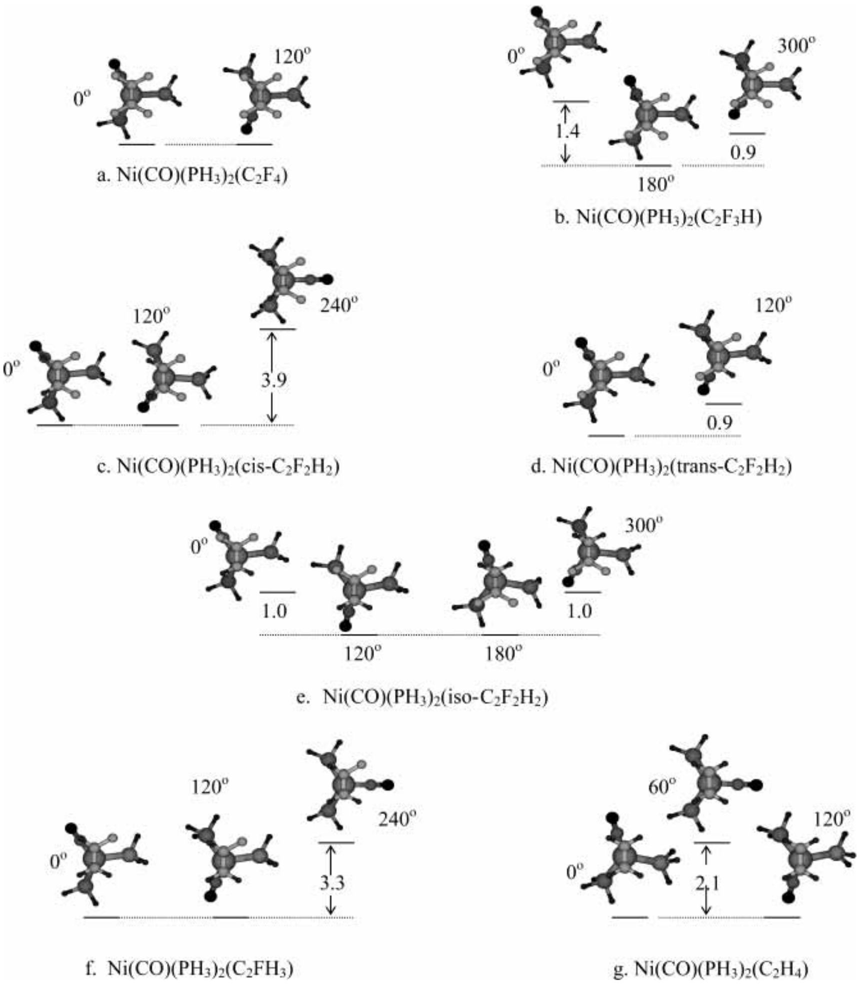
a. Ni(CO)(PH$_3$)$_2$(C$_2$F$_4$)

b. Ni(CO)(PH$_3$)$_2$(C$_2$F$_3$H)

c. Ni(CO)(PH$_3$)$_2$(cis-C$_2$F$_2$H$_2$)

d. Ni(CO)(PH$_3$)$_2$(trans-C$_2$F$_2$H$_2$)

e. Ni(CO)(PH$_3$)$_2$(iso-C$_2$F$_2$H$_2$)

f. Ni(CO)(PH$_3$)$_2$(C$_2$FH$_3$)

g. Ni(CO)(PH$_3$)$_2$(C$_2$H$_4$)

CHART 4

a. $Ni(CO)(PH_3)_2(C_2Cl_4)$

b. $Ni(CO)(PH_3)_2(C_2Cl_3H)$

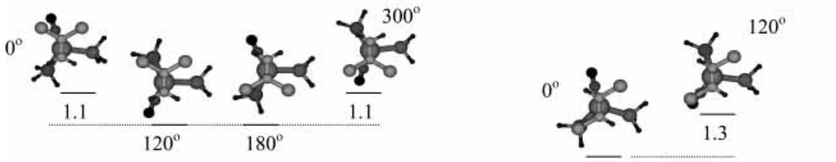

c. $Ni(CO)(PH_3)_2(iso\text{-}C_2Cl_2H_2)$

d. $Ni(CO)(PH_3)_2(trans\text{-}C_2Cl_2H_2)$

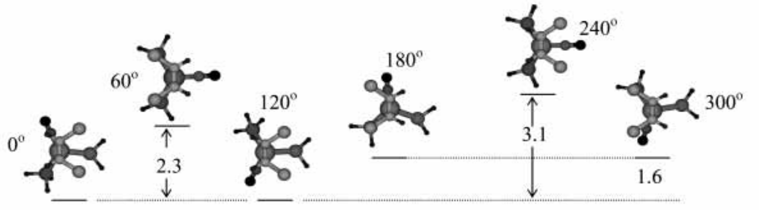

e. $Ni(CO)(PH_3)_2(cis\text{-}C_2Cl_2H_2)$

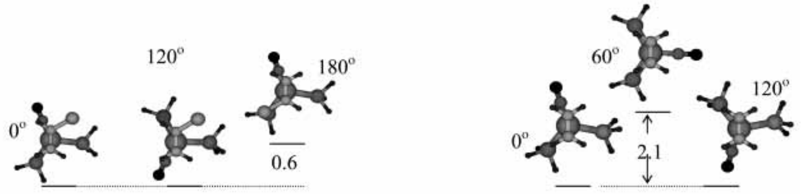

f. $Ni(CO)(PH_3)_2(C_2ClH_3)$

g. $Ni(CO)(PH_3)_2(C_2H_4)$

TABLE 4: Calculated Ni−Olefin Bond Energies (Δ*E*) and Enthalpies (Δ*H*, in parentheses for lowest energy isomers) for $Ni(PH_3)_2(CO)(C_2X_nH_{4-n})$ (X = F, Cl; *n* = 0−4) Complexes[a]

olefin	0°	60°	120°	180°	240°	300°
C_2F_4	20.4 (16.5)	*	20.4			
C_2F_3H isomer a	16.9	*	*	18.3 (16.4)	*	17.4
C_2F_3H isomer b	*	*	16.9	17.4	*	18.3
i-$C_2F_2H_2$	13.8	*	14.8 (11.6)			
t-$C_2F_2H_2$ isomer a	17.4 (15.3)	*	16.6			
t-$C_2F_2H_2$ isomer b	16.7	*	17.5			
c-$C_2F_2H_2$	17.4 (14.6)	*	17.4	*	13.5	*
C_2FH_3 isomer a	*	13.0	*	16.2 (12.7)	*	16.3
C_2FH_3 isomer b	16.2	*	16.1	*	12.9	*
C_2Cl_4	20.4 (19.4)	*	20.4			
C_2Cl_3H isomer a	*	*	18.8	20.5 (19.7)	*	19.6
C_2Cl_3H isomer b	18.9	*	*	19.9	*	20.6
i-$C_2Cl_2H_2$	18.5	*	19.6 (17.0)			
t-$C_2Cl_2H_2$ isomer a	17.3 (14.4)	*	16.0			
t-$C_2Cl_2H_2$ isomer b	16.1	*	17.3			
c-$C_2Cl_2H_2$	16.4 (13.1)	14.1	16.4	14.8	13.3	14.3
C_2ClH_3 isomer a	*	*	16.1	16.8 (13.1)	*	16.4
C_2ClH_3 isomer b	16.8	*	16.8	16.2	*	*
C_2H_4	17.6 (13.8)	15.5	17.6			

[a] In kcal/mol. Refer to Chart 1 for notation used to label isomers and Charts 3 and 4 for structures. Isomer b is the enantiomer of isomer a. An * indicates that a rotamer converted to the closest lower energy isomer obtained by rotation of the olefin.

(see Charts 3b and 4b). However, there is still one halogen that could be eclipsing either CO or PH_3. Interestingly, the isomer in which the halogen is eclipsing the phosphine ligand is ∼1 kcal/mol more stable than the one in which the halogen is eclipsing the CO ligand. This difference can be attributed to steric interactions between the electrons in the π system of the triple bond in the CO ligand and the lone pair electrons in the p orbitals of the halogen. The rotamer with two halogens eclipsing each a CO and PH_3 is the highest energy isomer that is a minimum on the potential energy surface and is ∼1.5−2 kcal/mol higher in energy than the lowest one, meaning that the eclipsed interaction between a phosphines ligand and a halogen destabilizes the molecule by an additional 0.5−1 kcal/mol.

Complexes containing an iso-$C_2X_2H_2$ olefin have two equivalent minimum energy rotamers (120° and 180°), in which one of the halogens is eclipsing a phosphine ligand rather than the CO ligand (Charts 3e and 4c). Consistent with the results found for the trihalogenated olefin complexes, a rotamer in which the halogen is eclipsing the CO ligand is about 1 kcal/mol above the minimum energy rotamer. Similar results are found in the case of the trans-$C_2X_2H_2$ olefin complexes, where there is a pair of low-energy rotamers (and enantiomers), the lower being the one with the halogen eclipsing a phosphine ligand, while the one in which the halogen eclipses the carbonyl ligand is ~1 kcal/mol above (Charts 3d and 4d). In the case of the cis-$C_2X_2H_2$ complexes, there are some differences in terms of whether the halogen is fluorine or chlorine. In the case of fluorine (Chart 3c), the olefin positions in such a way that the fluorine atoms avoid being eclipsed by any other ligand. The 240° rotamer, in which the CO ligand is perpendicular to the C═C bond (i.e., is positioned between the two halogens), is 3.9 kcal/mol above the two other isomers in which the carbonyl ligand is away from the fluorines. This is one of the few cases in which a 60° or 240° rotamer converged to a minimum energy. For the cis-$C_2Cl_2H_2$ complexes, all of the six rotamers converged to minimum energy. In the two lowest energy rotamers (0° and 120°, which are enantiomers) the olefin is positioned such that both chlorines avoid being eclipsed with the other ligands. At about 1.6 kcal/mol above there are a pair of enantiomers (180° and 300°) in which the halogens are eclipsing a CO and a PH_3 ligand each, although the olefin is slightly rotated to avoid a full eclipsing of the halogen and CO. There are also a 60° and a 240° rotamer, 2.3 and 3.1 kcal/mol above the minimum energy rotamers, respectively. Interestingly, the 60° rotamer in which both halogens are eclipsing a phosphine ligand each is lower in energy than the 240° rotamer in which the halogens are staggered relative to the CO ligand. This indicates that whenever possible the lone pairs of the halogens will avoid the π system of the carbonyl ligand. The main reason as to why only the chlorinated cis-olefin complex yields all the rotamers as local minimum on the potential energy surface while the fluorinated cis-olefin complex does not is that the steric bulk of chlorine atoms forces the other ligands to bend away from the olefin. Thus, both PH_3 and CO are relatively far from cis-$C_2Cl_2H_2$ in comparison to cis-$C_2F_2H_2$, as evidenced by the P−Ni−P angles and Ni−C_{olefin} bond lengths (see Table 3).

The monohalogenated olefin complexes (Charts 3f and 4f) also show slight differences depending on whether the halogen is fluorine or chlorine. In both cases the lowest isomers are the pair of rotamers (0° and 120°, and their enantiomers) in which the only halogen in the olefin avoids eclipsing interactions with the other ligands. For the fluorinated complex, the 240° rotamer is the only other energy minimum rotational isomer at 3.3 kcal/mol above the lower energy ones. This conformation of the complex resembles that of the 240° cis-$C_2F_2H_2$ rotamer, in which fluorine atoms avoid being eclipsed by any other ligand. For the C_2ClH_3 complex, the only other energy minimum rotamer is the 180°, which is ~0.6 kcal/mol above the lowest energy. In this conformer the chlorine avoids being eclipsed or staggered with the CO ligand, consistent with the conformations of the cis-$C_2Cl_2H_2$ complexes.

Discussion

Ni−Olefin Bond Strengths as a Function of the Number of Halogens in the Olefin. To simplify the analysis of the effect of the electron-withdrawing ability of the olefin in the nickel−olefin bond strength, only the rotamers of lowest energy were considered. According to the common qualitative interpretation of the DCD model for metal−olefin binding, an increase in the electron-withdrawing capability of the olefin should result in a stronger metal−olefin bond, because the back-bonding interaction is increased. One way to increase and tune the electron-withdrawing ability of an olefin is by increasing the number of electronegative substituents around the double bond. Figure 1 shows plots of the calculated nickel−olefin bond enthalpies as a function of the number of halogens. As can be seen, the metal−olefin bond strength does not seem to be affected much when the electron-withdrawing capability of the olefin is increased. The nickel−olefin bond dissociation energy does not show a strong dependence on the identity of the halogen and the number of halogens around the C═C bond. The bond energy slightly decreases when one halogen is introduced and then slightly increases with increasing the number of halogens, but at the end bond strengths do not differ by more than 5 kcal/mol. These results are consistent with the experimental nickel−fluoroolefin bond dissociation energies estimated by Tolman[22] from equilibrium studied in (olefin)bis(tri-*o*-tolyl phosphite)-nickel complexes (Figure 1).

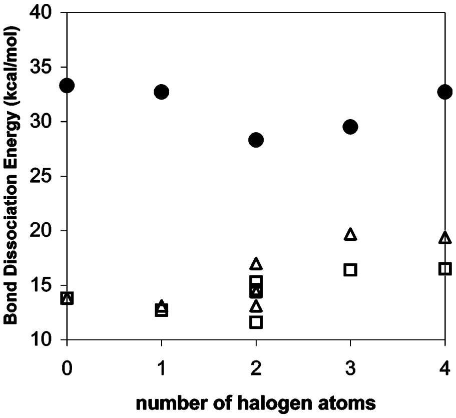

Figure 1. Plot showing the dependence of the nickel−olefin bond dissociation energy as a function of the number of halogens in the olefin: (□) calculated for $Ni(CO)(PH_3)_2(C_2F_nH_{4-n})$; (△) calculated for $Ni(CO)(PH_3)_2(C_2Cl_nH_{4-n})$; (●) experimental estimate from ref 22 for $Ni\{P(O\text{-}o\text{-tolyl})_3\}_2(C_2F_nH_{4-n})$.

To analyze why the nickel−olefin bond strength does not increase as the electron-withdrawing capability of the olefin increases, a simple energy decomposition analysis (eq 4) was performed. Figure 2a,b shows plots depicting the nickel−olefin bond energy (ΔE) and its two components: the net interaction energy (ΔE_{int}) and the reorganizational energy (ΔE_{reorg}). These plots reveal that the magnitude of both the interaction energy and the reorganizational energy increases with an increase in the number of halogens around the double bond. It can be inferred that the overall bond strength does not change much because any increase in the attractive net interaction energy is opposed by the negative energy term due to the reorganization of both the olefin and the $Ni(CO)(PH_3)_2$ fragment. Interestingly both halogenated complex series behave similarly, because both interaction energies and reorganizational energies for a complex with a given number of halogens in the olefin are alike. It is then straightforward to conclude that the reorganization of the olefin and $Ni(CO)(PH_3)_2$ plays a determining role in the overall metal−olefin bond strengths in the series of complexes in this study.

Further decomposition of the reorganizational energy (ΔE_{reorg}) into two components, one due to the olefin (ΔE_{reorg}(olefin)) and one due to the $Ni(CO)(PH_3)_2$ complex (ΔE_{reorg}(complex)), is possible:

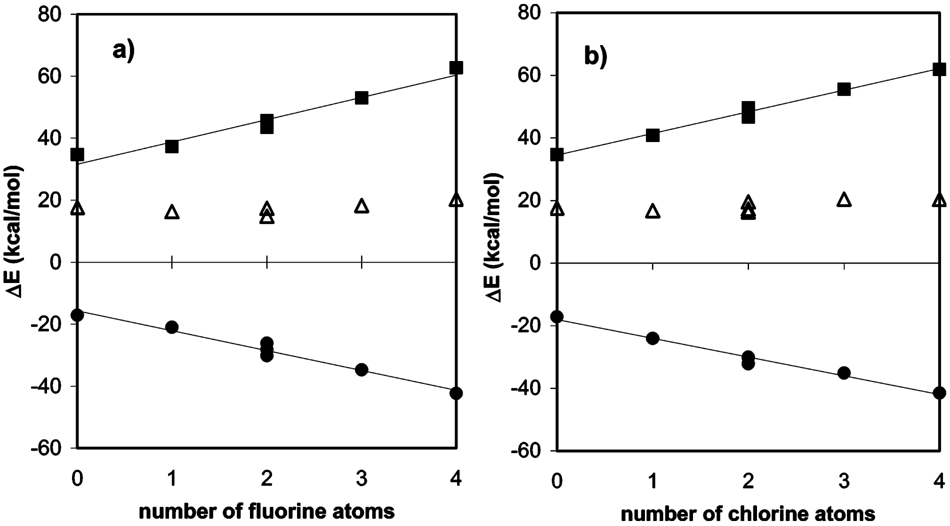

Figure 2. Plots showing the dependence of ΔE_{int} (■), ΔE_{reorg} (●), and ΔE (= $\Delta E_{\text{int}} + \Delta E_{\text{reorg}}$) (△) as a function of the number of halogens in the olefin: (a) calculated for $Ni(CO)(PH_3)_2(C_2F_nH_{4-n})$; (b) calculated for $Ni(CO)(PH_3)_2(C_2Cl_nH_{4-n})$.

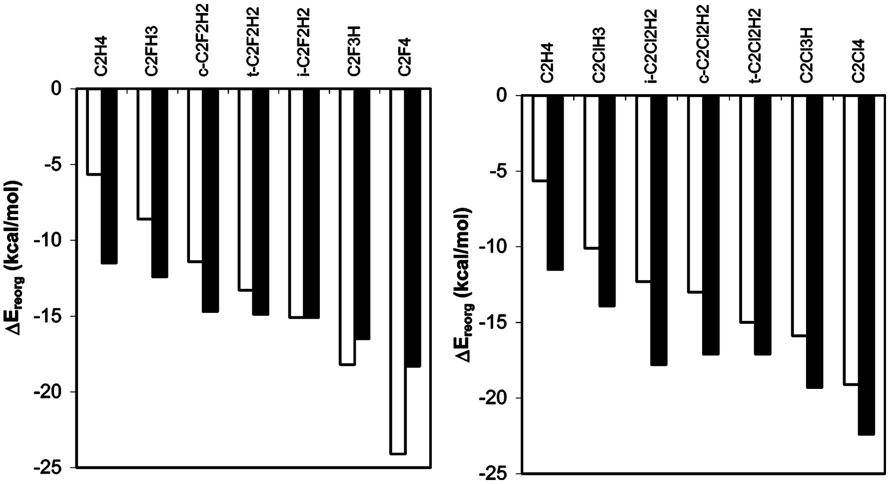

Figure 3. Bar graphs showing reorganizational energy terms (according to eq 5) for olefin (white bars) and $Ni(CO)(PH_3)_2$ (solid bars). Left graph for fluoroolefin complexes and right graph for chloroolefin complexes.

$$\Delta E_{\text{reorg}} = \Delta E_{\text{reorg}}(\text{olefin}) + \Delta E_{\text{reorg}}(\text{complex}) \qquad (5)$$

The results of such decomposition are shown in Figure 3 for each of the fluorinated and chlorinated series of complexes. It is clearly seen that the reorganization of both the olefin and $Ni(CO)(PH_3)_2$ contributes largely to the overall bond strength. The decomposition analysis reveals that both the olefin and the metal complex reorganization energies increase almost linearly with an increase in the number of halogens. However, in the fluorinated series, the contribution of the reorganization of a fluoroolefin to the total reorganization becomes more important than the reorganization of $Ni(CO)(PH_3)_2$ as the number of fluorines is increased. For instance, the reorganization of C_2F_4 releases 4.3 times more energy than ethylene, while reorganization of the $Ni(CO)(PH_3)_2$ complex upon olefin dissociation in $Ni(CO)(PH_3)_2(C_2F_4)$ releases only 1.6 times the energy that is required to reorganize the same fragment upon ethylene dissociation in $Ni(CO)(PH_3)_2(C_2H_4)$. The situation is rather different for the series of chlorinated olefin complexes. First a chlorinated olefin with a given number of halogens tends to deform slightly less than the corresponding fluoroolefin. For example, C_2F_4 releases 24 kcal/mol of energy, while C_2Cl_4 releases 19 kcal/mol upon reorganization. Second, the reorganization of the $Ni(CO)(PH_3)_2$ metal fragment becomes more important in the chlorinated series relative to the fluorinated series as the number of halogens increases. For instance, the reorganization of the metal fragment is 57% of the total reorganization in $Ni(CO)(PH_3)_2(C_2Cl_4)$, but it accounts for only 43% of the total reorganization of $Ni(CO)(PH_3)_2(C_2F_4)$.

Origin of Reorganizational Energies. In this section the origin and trends observed in the reorganizational energies are rationalized in terms of changes in the geometries and natural orbital populations. It is widely known that when an olefin is bonded to a metal, it is no longer planar (the olefin is said to be pyramidalized).[44] The pyramidalization of the olefin is due to sp^2 to sp^3 rehybridization resulting from both the reduction of electron density in the π HOMO and the increase of electron density in the π^* LUMO as a result of the σ and π metal−olefin bonding interactions. Upon bond dissociation, rehybridization of the olefin is manifested in a change in the angle of planarity (pyramidalization angle, Θ) of the olefin as each carbon is going from a quasi-tetrahedral (or pyramidal) geometry within the complex to a trigonal planar geometry in the ground state free olefin. In addition, the C=C bond order is increased from a value between 1 and 2 in the complex to 2 in the free olefin. The increase of the bond order implies that the carbon−carbon bond length decreases as a result of the bond dissociation. Therefore, if rehybridization is responsible for the reorganizational energy of the olefin, it is then expected that the

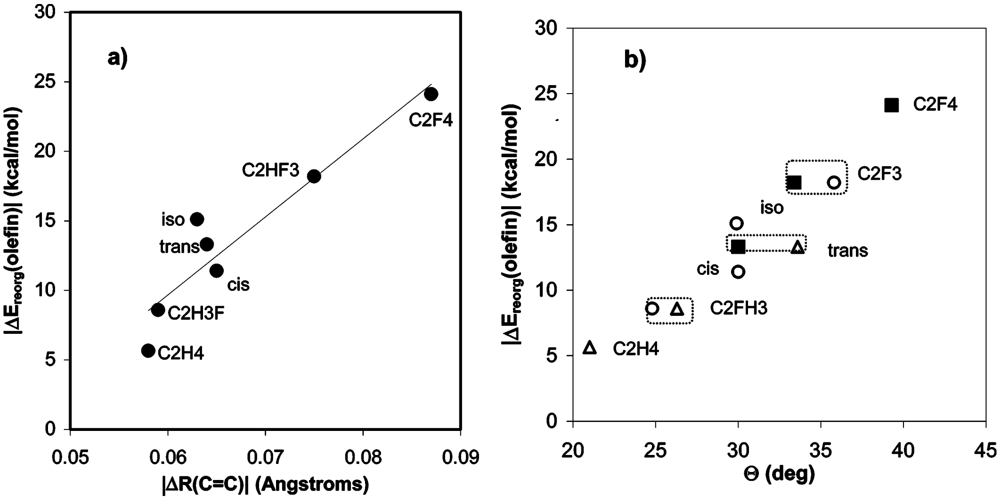

Figure 4. Plots showing the correlation between reorganizational energy in fluoroolefins ($\Delta E_{\mathrm{reorg}}$(olefin)) and (a) the change in the C−C bond length (●); (b) the pyramidalization angle (Θ) measured relative to the dihedral angles: H−C═C−H (△), H−C═C−F (●), F−C═C−F (■).

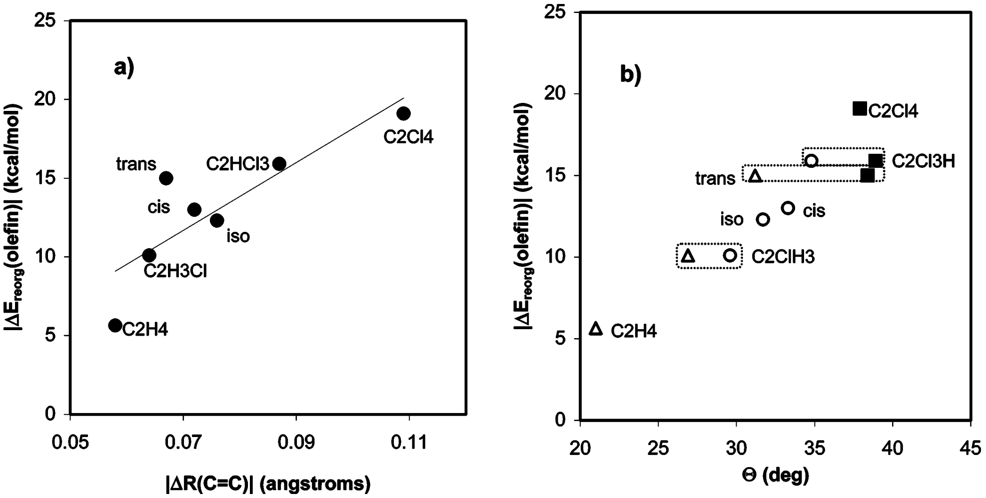

Figure 5. Plots showing the correlation between reorganizational energy in chloroolefins ($\Delta E_{\mathrm{reorg}}$(olefin)) and (a) the change in the C−C bond length (●); (b) the pyramidalization angle (Θ) measured relative to the dihedral angles: H−C═C−H (△), H−C═C−F (●), F−C═C−F (■).

reorganizational energy should correlate to the changes in both the C−C bond length and the pyramidalization angle. Figures 4 and 5 show plots of both the change of the C−C bond length and the Θ angle of the olefin versus the reorganization energy of the fluoro- and chloroolefins, respectively. Clearly, there is an almost linear correlation between these geometrical parameters and the reorganizational energy of the olefin. In terms of the change in the C═C bond length, there is a distinctive difference between ethylene and the halogenated olefins, which puts ethylene out of the linear trend. There are also deviations in the dihalogenated isomers, which seem contrary to the expectations; that is, an increase in bond length should imply an increase in the reorganizational energy. This can be understood, however, if one takes into account that the reorganization of the olefin is not exclusively a result of the rehybridization of the olefin (an electronic effect). The geometrical reorganization of the olefin is also affected by the repulsive interactions between the substituents around the double bond and the other ligands bonded to the metal (a steric effect). The pyramidalization angle (Θ) also increases linearly with an increase in the number of halogens in the olefin, although the pyramidalization angle relative to the Cl−C═C−Cl dihedral (Figure 5b, filled squares) has a constant value (~38−39°) independent of the number of chlorines in the olefin. This trend is not found when considering the corresponding angle (F−C═C−F) for fluorinated olefins (Figure 4b, filled squares). This apparent discrepancy is due to the fact that the pyramidalization of the olefin is not exclusively due to the rehybridization of the olefin. It also has a component that originates from the steric interactions between the substituents in the olefin and the other ligands (CO and PH_3), which is stronger in the chlorinated olefins than in the fluorinated olefins due to the large size of chlorine atoms.

As pointed out previously, rehybridization of the olefin is caused by the changes in the populations of the molecular orbitals directly involved in the carbon−carbon double bond, which are σ, π, π^*, and σ^*. The free olefin has four electrons in the bonding MOs and none in the antibonding MOs. When the olefin is bonded to the metal, the electron population of the π MO (P_π) is reduced as a result of the olefin→metal σ interaction, while the electron population in the π^* MO (P_{π^*}) increases as a result of the metal→olefin back-bonding interaction. It is then possible to calculate the bond order (BO) in each of the bonded olefins from the calculated natural orbital populations of the MOs:

$$\mathrm{BO} = 2 + P_\pi - P_{\pi^*} \tag{6}$$

A plot of the bond order versus reorganizational energies of the olefins (Figure 6) shows a linear correlation, confirming

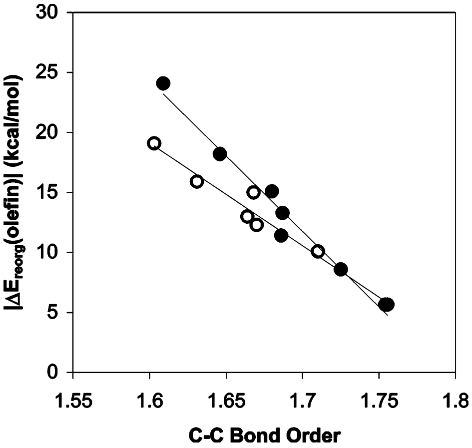

Figure 6. Plot showing the correlation between the calculated C−C bond order and reorganizational energy of fluoroolefins (●) and chloroolefins (○). The bond order decreases as the number of halogens in the olefin increases.

that reorganization of the olefin is proportional to the extent of rehybridization that the olefin undergoes when it interacts with the metal. Also, for a given series of halogenated olefin nickel complexes, an increase in the number of halogens in the olefin increases the rehybridization, which in turn increases the amount of reorganizational energy of the olefin (Figure 3).

The reorganization of the $Ni(CO)(PH_3)_2$ fragment is also an important factor in the overall reorganization of the complex, contributing between 40 and 70% to the total reorganizational energy, depending on the haloolefin complex under consideration. A partial contribution to the reorganization of this fragment is due to the fact that, upon olefin dissociation, the complex changes from a distorted tetrahedral-like geometry to a trigonal planar geometry in the ground state 16-electron $Ni(CO)(PH_3)_2$ complex. In addition to this, $Ni(CO)(PH_3)_2$ is further distorted in the olefin complex as a result of steric interactions between the ligands (CO and PH_3) and the substituents of the olefin. This distortion is manifested in the change in the P−Ni−P angle (see Table 3) and much clearer in the change in the sum of the P−Ni−P and the two OC−Ni−P angles (expressed as Ω, relative to 360° in the ground state $Ni(CO)(PH_3)_2$ complex). Figure 7 shows a plot of Ω versus the reorganizational energy of $Ni(CO)(PH_3)_2$. As expected, the distortion is larger as the number of halogens increases, with the increase being more pronounced for the chlorinated olefin complexes. There is an almost linear correlation for both the fluorinated and chlorinated series of olefin complexes, respectively. Deviations of the linear correlation may be attributed to the fact that the bending of the ligands away from the olefin is not the only geometrical change taking place in the $Ni(CO)(PH_3)_2$ fragment. There are also changes in the Ni−CO, Ni−P, and C−O bond lengths that differ from olefin to olefin. A comparison of reorganizational energies in $Ni(CO)(PH_3)_2$ between both olefin series also shows that the reorganization of the $Ni(CO)(PH_3)_2$ fragment is slightly larger for chlorinated complexes, in good agreement with the fact that chlorinated olefins distort this fragment more than fluorinated olefins do (Figure 7).

Comparisons to Other Systems. Recent studies have focused on the analysis of bond energy trends in different organometallic olefin complexes.[23−26,45−47] Among these studies, those by Weitz and co-workers,[23,26] Nunzi et al.,[24] and Massera and Frenking[47] have recognized the importance of reorganizational and steric effects in the metal−olefin bond strength. In their study of the series $M(PH_3)_2(C_2X_4)$ (M = Ni, Pd, Pt and X = H, F, CN) Nunzi et al. found that for M = Ni the $Ni-C_2X_4$ bond strength follows the trend $C_2(CN)_4 > C_2F_4 \approx C_2H_4$. Their results show that even though the net interactions of C_2F_4 with $Ni(PH_3)_2$ are stronger than those of C_2H_4, the Ni−olefin bond energy is about the same as a result of reorganizational and steric effects. Our results are in very good agreement with theirs. Furthermore, it can be inferred from their data that both $C_2(CN)_4$ and C_2F_4 have the same net interaction energy, but the smaller reorganization energy in $C_2(CN)_4$ accounts for the 12 kcal/mol difference between the calculated (and experimental) Ni−olefin bond strengths. Even though the complexes in this study and those in Nunzi et al. differ only by the presence of a CO ligand, the trends in both geometrical changes and bond strengths for X = H and F are similar (see Table 5 for a comparison of bond energy terms). The absolute differences in the energetic terms are expected. The difference of about 12−13 kcal/mol in bond energies (ΔE) can be accounted for by the difference in the interaction energy, perhaps arising from both less repulsive Pauli interactions and more attractive orbital interactions in the case of $Ni(PH_3)(C_2H_4)$, which lacks the carbonyl ligand. In fact, the presence of the carbonyl ligand increases the reorganizational energy of the $Ni(CO)(PH_3)_2$ fragment (to a larger extent in the C_2F_4 complex) likely due to the fact that steric interactions are larger in the presence of the carbonyl. This is manifested in the differences in P−Ni−P angles (109.7° for $Ni(PH_3)_2(C_2F_4)$ vs 105.1° for $Ni(CO)(PH_3)_2(C_2F_4)$). The presence of the carbonyl tends to decrease the reorganizational energy of the olefin by about 2 kcal/mol, likely because CO is a good back-bonding ligand and competes with the olefin for the metal's electron density.

Studies by Weitz and co-workers have focused on tetrahalogenated olefin complexes of iron and chromium carbonyls. Cedeño and Weitz[23] showed that for the series $Cr(CO)_5(C_2X_4)$, in which the experimental Cr−olefin bond energies follow the trend $C_2H_4 \approx C_2F_4 > C_2X_4$, both the reorganization of the olefin and Pauli electronic repulsions (steric) are responsible for the overall bond strength. This occurs despite that, from molecular orbital considerations alone, the strength of the olefin−$Cr(CO)_5$ interaction follows the trend $C_2F_4 > C_2Cl_4 > C_2H_4$, in agreement with the expectations derived from the DCD model. Our results seem to indicate that something similar occurs in the series of complexes studied here. The net interaction energy (ΔE_{int}, Figure 2) increases steadily with an increase in the number of electron-withdrawing substituents around the double bond, which means that the attractive orbital interactions between the olefin and the metal are increased with an increase in the number of halogens as the DCD model implies. However the neglect of the effect of reorganization and steric effects in the overall metal−olefin interaction may lead one to wrongly conclude that the actual bond dissociation energies or enthalpies (ΔE, ΔH) should follow the trend given by the orbital interaction energies (referred to as ΔE_{DCD} in ref 23).

Finally, our computational results are in good agreement with the experimental trend observed by Tolman[22] for the series of fluorinated olefin complexes $Ni\{P(O(o\text{-tolyl}))_3\}_2(C_2H_{4-n}F_n)$ (see Figure 1) and further reaffirm what Tolman intuitively (and accurately!) suggested in his classical study:

> The fluoroolefins behaved in a peculiar way. Increasing n in the series $C_2H_{4-n}F_n$ caused K_1 (the stability equilibrium constant) to decrease to a minimum and rise to a value comparable to that of C_2H_4 with C_2F_4.... The structural reorganization required before C_2F_4 can bond effectively may be responsible for the slowness of this reaction with NiL_3.... Our data suggest that the degree to

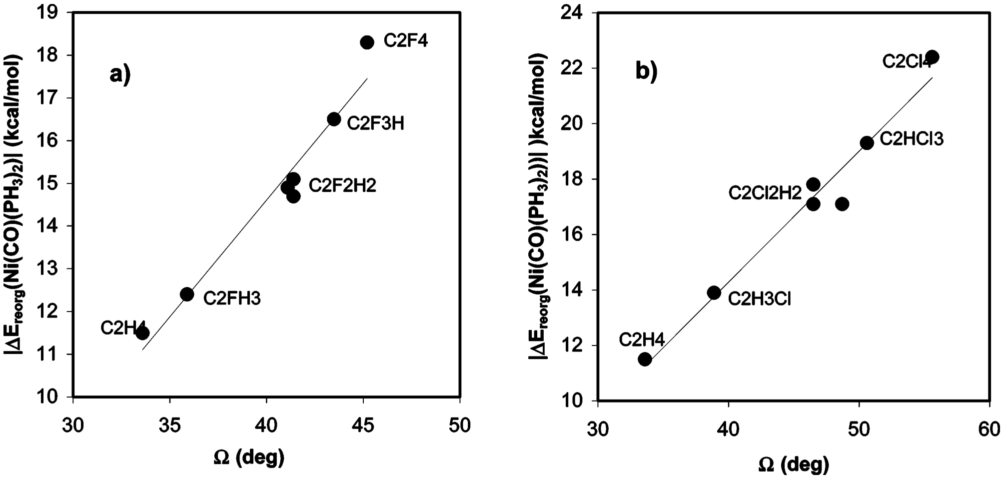

Figure 7. Plots showing the correlation between the reorganizational energy of $Ni(CO)(PH_3)_2$ and the sum of the angles between its ligands (Ω): (a) for the $Ni(CO)(PH_3)_2(C_2F_nH_{4-n})$ series; (b) for the $Ni(CO)(PH_3)_2(C_2Cl_nH_{4-n})$ series.

TABLE 5: Comparison of Ni−C_2X_4 Bond Energy Terms (in kcal/mol) for $Ni(PH_3)_2CO(C_2X_4)$ and $Ni(PH_3)_2(C_2X_4)$, X = H, F

	ΔE_{int}	ΔE_{reorg} (olefin)	ΔE_{reorg} (metal fragment)	ΔE
$Ni(PH_3)_2CO(C_2H_4)$[a]	34.8	−5.6	−11.5	17.6
$Ni(PH_3)_2(C_2H_4)$[b]	46.4	−7.1	−8.8	30.4
$Ni(PH_3)_2CO(C_2F_4)$[a]	62.7	−24.0	−18.3	20.4
$Ni(PH_3)_2(C_2F_4)$[b]	70.5	−26.3	−11	32.7

[a] This work. [b] Reference 24.

> which substituents are bent back away from the metal in transition metal olefin complexes is not simply related to the metal-olefin bond strengths. Tetraflurorethylene, which shows extreme bending back in other systems, shows a bond strength to Ni(0) which is not greater than, and probably less than, that of ethylene itself.

As pointed out in the previous section, reorganization of both the olefin and $Ni(CO)(PH_3)_2$ plays a determining role in the measurable metal−olefin bond strength. Paradoxically, the electron-withdrawing ability of the halogens increases the extent of the orbital interaction of the olefin with the metal (by increasing the back-bonding) but at the same time induces energy-costly reorganizations in the olefin (mainly by rehybridization) and the metal fragment (dependent on the extent of repulsive interactions with other ligands). In the case of the series of halogenated complexes studied here and by Tolman, such reorganizational energy is costly enough to decrease the net attractive interaction energy, such that the nickel−haloolefin bond strength is similar to the nickel−ethylene bond strength.

Conclusion

A density functional study (BP86/LACV3P**) of electron-withdrawing effects on the metal−olefin bond strengths in the series of complexes $Ni(PH_3)_2(CO)(C_2X_nH_{4-n})$ (X = F, Cl; n = 0−4) has been performed. Rotational isomers were considered for a given n. The lowest energy rotamer, in all cases, prefers to have a PH_3 ligand staggered to the C−C axis of the olefin and avoids an eclipsing interaction between a halogen and the CO ligand. Bond energy calculations indicate that the Ni−olefin bond strength is not largely affected by the electron-withdrawing capability of the olefin, which increases with an increase in the number and electronegativity of halogens (F, Cl) around the double bond. This trend is in agreement with experimental observations by Tolman[22] for the $Ni\{P(O(o\text{-tolyl}))_3\}_2(C_2H_{4-n}F_n)$ series of complexes. A simple bond energy decomposition scheme has been used to explain this “unexpected” trend from the point of view of the commonly used Dewar−Chatt−Duncanson (DCD) model for metal−olefin bonding. The decomposition analysis reveals that even though the net interaction energy between the metal and the olefin increases with an increase in the number of halogens (in agreement with the DCD model), the energy released in the reorganization of both the olefin and $Ni(CO)(PH_3)_2$ 16-electron metal complex to their respective ground state conformations also increases with an increase in the electron-withdrawing capability of the olefin. Given that the reorganizational energy is opposite in sign to the interaction energy, metal−olefin bond energies of complexes with olefins that are more electron withdrawing than ethylene do not necessarily have Ni−olefin bond strengths that are much larger than that of ethylene.

Acknowledgment. The authors thank the Chemistry Department, the College of Arts and Sciences, and the Office of the Provost at Illinois State University for their support. Acknowledgment is also made to the donors of the Petroleum Research Fund, administered by the ACS, for partial support of this research under grant 39604-GB3.

References and Notes

(1) Parshall, G. W. *Homogeneous Catalysis−The Applications and Chemistry of Catalysis by Soluble Transition Metals*; Wiley-Interscience: New York, 1980.

(2) Collman, J. P.; Hegedus, L. S.; Norton, J. R.; Finke, R. G. *Principles and Applications of Organotransition Metal Chemistry*; University Science Books: Mill Valley, CA, 1987.

(3) Pruchnick, F. P. *Organometallic Chemistry of the Transition Elements*; Plenum: New York, 1990.

(4) *Catalytic Asymmetric Synthesis*, 2nd ed.; Ojima, I., Ed.; Wiley-VCH: New York, 2000.

(5) Crabtree, R. H. *The Organometallic Chemistry of Transition Metals*, 3rd ed.; Wiley: New York, 2001.

(6) Grevels, F. W.; Lindemann, M.; Benn, R.; Goddard, R.; Krueger, C. *Z. Naturforsch., B: Anorg. Chem., Org. Chem.* **1980**, *35B*, 1298.

(7) Kazlauskas, R. J.; Wrighton, M. S. *J. Am. Chem. Soc.* **1982**, *104*, 6005.

(8) Miller, M. E.; Grant, E. R. *J. Am. Chem. Soc.* **1984**, *106*, 4635.

(9) Wuu, Y. M.; Bentsen, J. G.; Brinkley, C. G.; Wrighton, M. S. *Inorg. Chem.* **1987**, *26*, 530.

(10) Barnhardt, T. M.; McMahon, R. J. *J. Am. Chem. Soc.* **1992**, *114*, 5434.

(11) Maxwell, J. L.; Brown, K. C.; Bartley, D. W.; Kodadek, T. *Science* **1992**, *256*, 1544.

(12) Long, G. T.; Wang, W.; Weitz, E. *J. Am. Chem. Soc.* **1995**, *117*, 12810.

(13) Szymańska-Buzar, T.; Jaroszewski, M.; Wilgocki, M.; Ziółkowski, J. J. *J. Mol. Catal. A* **1996**, *112*, 203.

(14) Long, G. T.; Weitz, E. *J. Am. Chem. Soc.* **2000**, *122*, 1431.

(15) Carpentier, J.-F.; Wu, Z.; Lee, C. W.; Stroemberg, S.; Cristopher, J. N.; Jordan, R. F. *J. Am. Chem. Soc.* **2000**, *122*, 7750.

(16) Dewar, M. J. S. *Bull. Chem. Soc. Fr.* **1951**, *18*, C71.

(17) Chatt, J.; Duncanson, L. A. *J. Chem. Soc.* **1953**, 2939.

(18) Mingos, D. M. P. *J. Organomet. Chem.* **2001**, *635*, 1.

(19) See ref 3, Chapter 6, p 343.

(20) See ref 5, Chapter 5, p 116.

(21) Cramer, R. *J. Am. Chem. Soc.* **1967**, *89*, 4621.

(22) Tolman, C. A. *J. Am. Chem. Soc.* **1974**, *96*, 2780.

(23) Cedeño, D. L.; Weitz, E. *J. Am. Chem. Soc.* **2001**, *123*, 12857.

(24) Desmarais, N.; Adamo, C.; Panunzi, B.; Barone, V.; Giovannitti, B. *Inorg. Chim. Acta* **1995**, *238*, 159.

(25) Nunzi, F.; Sgamelotti, A.; Re, N., Floriani, C. *J. Chem. Soc., Dalton Trans.* **1999**, 3487.

(26) Cedeño, D. L.; Weitz, E.; Bérces, A. *J. Phys. Chem. A* **2001**, *105*, 8077.

(27) *Jaguar 4.1*; Schrödinger, Inc.: Portland, OR, 1991−2000.

(28) All methods use the Slater local exchange functional: Slater, J. C. *Quantum Theory of Molecules and Solids, Vol. 4: The Self-Consistent Field for Molecules and Solids*; McGraw-Hill: New York, 1974.

(29) B3LYP uses a three-parameter hybrid method by Becke: Becke, A. D. *J. Chem. Phys.* **1993**, *98*, 5648.

(30) All methods use the gradient correction to exchange by Becke: Becke, A. D. *Phys. Rev. A* **1988**, *38*, 3098.

(31) BP86 and BLYP use the local correlation functional by Perdew and Zunger: Perdew, J. P.; Zunger, A. *Phys. Rev. B* **1981**, *23*, 5048.

(32) B3LYP uses the VWN local correlation: Vosko, S. H.; Wilk, L.; Nusair, M. *Can. J. Phys.* **1980**, *58*, 1200.

(33) BLYP and B3LYP use the LYP gradient-corrected correlation functional: (a) Lee, C.; Yang, W.; Parr, R. G. *Phys. Rev. B* **1988**, *37*, 785. (b) Miehlich, B.; Savin, A.; Stoll, H.; Preuss, H. *Chem. Phys. Lett.* **1989**, *157*, 200.

(34) BP86 uses the gradient-corrected correlation functional by Perdew: (a) Perdew, J. P. *Phys. Rev. B* **1986**, *33*, 8822. (b) Perdew, J. P. *Phys. Rev. B* **1986**, *34*, 7406.

(35) Hay, P. J.; Wadt, W. R. *J. Chem. Phys.* **1985**, *82*, 299.

(36) (a) Clark, T.; Chandrasekhar, J.; Spitznagel, G. W.; Schleyer, P. von R. *J. Comput. Chem.* **1983**, *4*, 294. (b) Frisch, M. J.; Pople, J. A.; Binkley, J. S. *J. Chem. Phys.* **1984**, *80*, 3265. (c) Krishnan, R.; Binkley, J. S.; Seeger, R.; Pople, J. A. *J. Chem. Phys.* **1980**, *72*, 650. (d) McLean, A. D.; Chandler, G. S. *J. Chem. Phys.* **1980**, *72*, 5639.

(37) Glendening, E. D.; Badenhoop, J. K.; Reed, A. E.; Carpenter, J. E.; Weinhold, F. *NBO 4.0*; Theoretical Chemistry Institute, University of Wisconsin: Madison, WI, 1996.

(38) Turner, J. J.; Simpson, M. B.; Poliakoff, M., Maier, W. B., II. *J. Am. Chem. Soc.* **1983**, *105*, 3898.

(39) Stevens, A. E.; Feigerle, C. S.; Lineberger, W. C. *J. Am. Chem. Soc.* **1982**, *104*, 5026.

(40) Brown, C. E.; Mitchell, S. A.; Hackett, P. A. *Chem. Phys. Lett.* **1992**, *191*, 175.

(41) Cedeño, D. L.; Weitz, E.; Bérces, A. *J. Phys. Chem. A* **2001**, *105*, 3773.

(42) Cheng, P. T.; Cook, C. D.; Koo, C. H.; Nyburg, S. C.; Shiomi, M. T. *Acta Crystallogr. B* **1971**, *27*, 1904.

(43) Krüger, C.; Tsay, Y.-H. *Cryst. Struct. Commun.* **1974**, *3*, 455.

(44) For example, see ref 2, Chapter 3, p 150.

(45) Frenking, G.; Pidun, U. *J. Chem. Soc., Dalton Trans.* **1997**, 1653.

(46) Cedeño, D. L.; Weitz, E. *J. Phys. Chem. A* **2002**, *106*, 4651.

(47) Massera, C.; Frenking, G. *Organometallics* **2003**, *22*, 2758.